

## Antioxidant Chemistry: Hypotaurine–Taurine Oxidation by Chlorite<sup>1</sup>

Bice S. Martincigh

Department of Chemistry and Applied Chemistry, University of Natal, Private Bag X10, Dalbridge 4014, Republic of South Africa

Claudius Mundoma and Reuben H. Simoyi\*

Department of Chemistry, West Virginia University, Morgantown, West Virginia 26506-6045

Received: June 10, 1998; In Final Form: September 24, 1998

Extensive experimental data have been collected on the oxidation of hypotaurine,  $\text{H}_2\text{NCH}_2\text{CH}_2\text{SO}_2\text{H}$ , by chlorite and chlorine dioxide. Hypotaurine is stable and reacts slowly with chlorite to give taurine, hypotaurine sulfonic acid, and monochloro- and dichlorotaurine. However, it reacts rapidly with chlorine dioxide with a second-order rate constant of  $801 \text{ M}^{-1} \text{ s}^{-1}$  to give taurine. Oxidation occurs simultaneously at the sulfur center (to give the sulfonic acid) and at the nitrogen center (to give the chloramines). The stoichiometry of the reaction was experimentally determined to be  $\text{ClO}_2^- + \text{H}_2\text{NCH}_2\text{CH}_2\text{SO}_2\text{H} + \text{H}^+ \rightarrow \text{ClHNCH}_2\text{CH}_2\text{SO}_3\text{H} + \text{H}_2\text{O}$ . The formation of dichlorotaurine is favored only in high acid environments.

### Introduction

Although the physiological roles antioxidants play in the human body have been studied<sup>2</sup> extensively, *in vitro* antioxidant chemistry studies are still in their infancy. There is a need to study mechanistic details of how antioxidants protect tissue from harmful oxidants. A good start would be to identify common antioxidants and study their reactivity patterns *in vitro*.

The biochemistry and clinical biology communities have different definitions of an antioxidant.<sup>3</sup> In this paper, we will assume that an antioxidant is a substance that, when present in low concentrations, can significantly delay oxidation of an oxidizable substrate.<sup>4</sup> Previous work suggests that hypotaurine and taurine fall into this category. A number of reactive oxygen species ( $\cdot\text{OH}$  and  $\text{O}_2\cdot^-$ ) are produced *in vivo*, and they oxidize and damage normal tissue.<sup>5</sup>  $\cdot\text{OH}$  can easily be produced in biological systems by the metal-ion-dependent decomposition of hydrogen peroxide.<sup>6</sup> Antioxidants should be able to scavenge all reactive oxygen species (ROS) and thus protect tissue from damage and also to reduce inflammation.<sup>7</sup>

The major antioxidants most commonly mentioned (cysteine, glutathione, taurine, hypotaurine, vitamin E, ascorbic acid, superoxide dismutase, and caeruloplasmin)<sup>8</sup> all contain an amino group. The formation of *N*-chloro- and *N*-bromamines has been suggested as possible mechanisms by which the most common harmful oxidants, HOCl and HOBr, can be scavenged.<sup>9</sup> With the high concentrations of  $\text{Cl}^-$  (0.10 M) and  $\text{Br}^-$  (0.001 M) in the human body, HOCl and HOBr can be easily produced from the myeloperoxidase-catalyzed peroxidation of chloride and bromide ions, respectively.<sup>10</sup> These neutrophil-derived prooxidants, HOCl and HOBr, are important in bacterial killing but also damage tissue at inflammation sites.<sup>11</sup>

A recent study showed that cephalosporins are scavengers of HOCl.<sup>12</sup> Even some cephalosporins without a primary amino group (such as cefamandole) have been shown to have powerful antioxidant activity with respect to HOCl, leading to a reduced antibiotic activity of the cephalosporin.<sup>13</sup> Cephalosporins contain thioether groups: speculation is that these groups may

be responsible for mopping up HOCl.<sup>12</sup> Specific studies are thus needed for each suspected antioxidant compound before its mechanism for antioxidant activity can be deduced.

Apart from its antioxidant activity, taurine has been implicated in several other physiological roles.<sup>14</sup> However, there is no adequate mechanistic data on how it functions in these roles. Most reports on mechanistic studies are speculative. For example, it has been reported that in physiological concentrations taurine can, *in vitro*, kill schistosoma mansoni.<sup>15</sup> Also, taurine has been shown to inhibit calcium-activated respiration in small mammalian liver mitochondria,<sup>16</sup> to inhibit nerve impulses in nerve tissues,<sup>17</sup> and to reduce cholesterol in vertebrates.<sup>18</sup>

Taurine and hypotaurine are closely linked. Taurine, with its special stability, is considered a metabolic end product of methionine and cysteine.<sup>19</sup> Most metabolic pathways give hypotaurine as a precursor to taurine.<sup>19</sup> Hypotaurine differs from taurine only in the oxidation state of the sulfur center and the resulting change in the acidity of the molecule.

In general, hypotaurine is much more reactive than taurine. Recent experimental data have shown that hypotaurine reacts rapidly and efficiently with the hydroxyl radical, superoxide radical, and hydrogen peroxide.<sup>20</sup> The ability to scavenge these reactive oxygen species rapidly is a prerequisite for a molecule to act as an antioxidant *in vivo*.<sup>21</sup> The other metabolic precursors of taurine, cysteic acid and cysteamine, are also poor scavengers of ROS as is taurine. Taurine also appears to be inefficient in moderating HOCl toxicity because the *N*-chloramine produced can still deactivate  $\alpha_1$ -antiproteinase.<sup>22</sup>

Some of our recent work examined the reactivity of taurine.<sup>23</sup> We found taurine to be extremely inert and surprisingly inactive to oxidation by the reactive radical oxyhalogen species  $\text{ClO}_2$  and by acidified bromate.<sup>23</sup> It did appear that, whatever physiological roles taurine might play, it does not seem to be a strong and effective antioxidant.

In this paper we report an extensive kinetics and mechanistic study of the reaction of hypotaurine with chlorite and chlorine

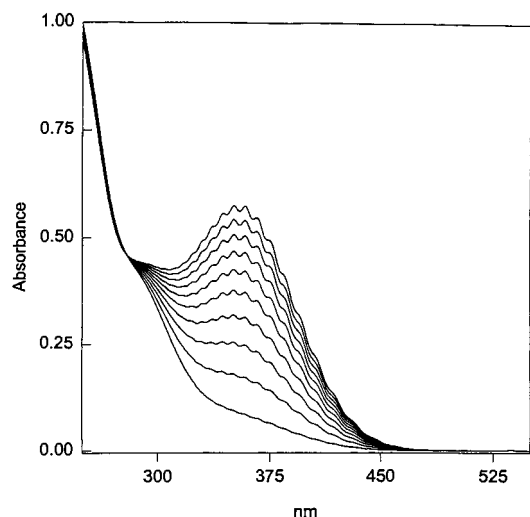


**Figure 1.** UV-vis spectral scans (60 s intervals) of the  $\text{ClO}_2^-$ –hypotaurine reaction. Absorbance readings are observed only at  $\lambda = 360$  nm, the absorption maximum wavelength for chlorine dioxide.  $[\text{ClO}_2^-]_0 = 1.01 \times 10^{-2}$  M;  $[\text{H}_2\text{NCH}_2\text{CH}_2\text{SO}_2\text{H}]_0 = 9.99 \times 10^{-4}$  M.

dioxide. A full mechanistic study of hypotaurine's reactivity can help in inferring to its reactivity *in vivo*.

### Experimental Section

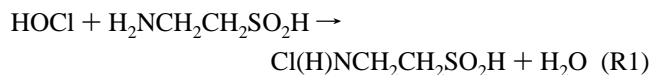
**Materials.** The following reagent-grade chemicals were used without further purification: hypotaurine (Aldrich), potassium iodide, sodium thiosulfate, and perchloric acid (69–72%) (Fisher). Sodium perchlorate solution was first filtered and then recrystallized twice from deionized water before use. Sodium chlorite was first recrystallized to approximately 96% assay before being used. Fresh sodium chlorite solutions were prepared before each set of experimental data was acquired. Chlorine dioxide was prepared by a method previously described.<sup>24</sup> It was standardized by its absorptivity coefficient of  $1265 \text{ M}^{-1} \text{ cm}^{-1}$  at 360 nm.

**Methods.** Product identification was by UV, IR, and  $^1\text{H}$  NMR spectroscopy. The proton NMR spectra were obtained on a JEOL GX 270 spectrometer using  $\text{D}_2\text{O}$  as the solvent and internal standard. Kinetics experiments were carried out at  $25 \pm 0.5$  °C and an ionic strength of 0.50 M ( $\text{NaClO}_4$ ). The reactions were followed spectrophotometrically using the absorbance of  $\text{ClO}_2$  at 360 nm. The slower reactions of chlorite and hypotaurine were followed on a Perkin-Elmer Lambda 2S UV/vis spectrophotometer, while the faster reactions of  $\text{ClO}_2$  and hypotaurine were followed on a Hi-Tech Scientific SF-61AF stopped-flow spectrophotometer.

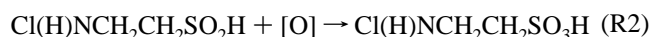
### Results

**Product Identification.** Taurine and hypotaurine do not absorb in the visible region of the spectrum. Chlorotaurine has a weak absorption at 250 nm. Figure 1 shows that  $\text{ClO}_2^-$ –hypotaurine mixtures give a featureless spectrum between 200 and 500 nm. The only signal in the visible region is the absorbance of chlorine dioxide at 360 nm.  $^1\text{H}$  NMR spectral data were sufficient to conclude that hypotaurine is oxidized to taurine, which is in turn further oxidized to *N*-chlorotaurine. Figure 2 shows NMR spectra of the substrate as well as its progressive transformation to chlorotaurine. Hypotaurine itself has a proton NMR spectrum shown in Figure 2a with two triplets that are displaced to low field with respect to taurine. These triplets integrate as two protons each. The positions of the triplets in hypotaurine and taurine are also heavily dependent

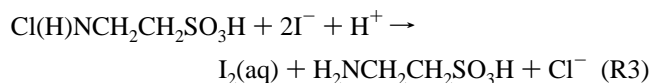
on the pH of the solution, and so all the spectra shown in Figure 2 were run in  $\text{DClO}_4$ . Upon mixing a 1:2 mole ratio of  $\text{ClO}_2^-$  to hypotaurine, the spectrum in Figure 2b is obtained. Two new sets of triplets appear, with one set centered at positions  $\delta = 3.24$  and the other at 3.05 (indicative of taurine and/or chlorotaurine). The NMR spectra of taurine and chlorotaurine are nearly identical. The other set of triplets are centered at  $\delta = 4.2$  and 3.55. Further addition of chlorite shows the progressive decrease in the intensity of this set of protons. This is shown in the series of spectra b, c, and d. In Figure 2d, excess chlorite effectively wipes out these triplet sets of protons. The only product left in the reaction mixture is chlorotaurine. The spectrum shown in Figure 2e is acidified taurine ( $\text{DClO}_4$ ) which has been added for comparison with the reaction product spectrum. The transient peaks in spectra b and c are due to the *N*-chlorination of the hypotaurine before it has been oxidized to taurine:



As the oxidation proceeds, the *N*-chlorohypotaurine,  $\text{Cl(H)NCH}_2\text{CH}_2\text{SO}_2\text{H}$ , is oxidized to *N*-chlorotaurine,  $\text{Cl(H)NCH}_2\text{CH}_2\text{SO}_3\text{H}$ , and the peaks gradually disappear:

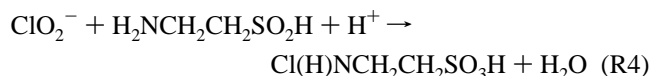


In conditions of excess  $\text{ClO}_2^-$ , the remaining chlorite could be quantitatively determined by using excess acidified iodide and titrating the liberated iodine with thiosulfate after correcting for the contribution from *N*-chloramine.<sup>25</sup> In excess hypotaurine the released *N*-chloramine could also be quantitatively determined by adding acidified iodide (as well) and analyzing for iodine.<sup>26</sup>

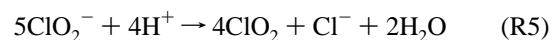


The reaction presents very little in terms of possible side reactions, and we confirmed only *N*-chlorotaurine ( $^1\text{H}$  NMR spectra),  $\text{ClO}_2$  (spectrophotometry,  $\lambda = 360$  nm), and  $\text{Cl}^-$  (gravimetric analysis and after prolonged standing) as the products of the reaction in excess  $\text{ClO}_2^-$ .

**Stoichiometry.** The stoichiometry of the chlorite–hypotaurine reaction was established as



The stoichiometry was obtained by running a series of experiments with excess  $\text{ClO}_2^-$  and measuring the  $\text{ClO}_2$  obtained after 12 days of incubation. Any excess  $\text{ClO}_2^-$  will be converted to  $\text{ClO}_2$  after all hypotaurine has been consumed with the stoichiometry:<sup>27</sup>



Required stoichiometry is when no production of  $\text{ClO}_2$  is observed at the highest possible ratio of the oxidant. Any further addition of chlorite above that required for stoichiometry R4 will result in excess chlorite, which will show up as chlorine dioxide according to stoichiometry R5. A plot of final absorbance of  $\text{ClO}_2$  (after an incubation period of 12 days) against the initial  $\text{ClO}_2^-$  concentrations gives a straight line with an

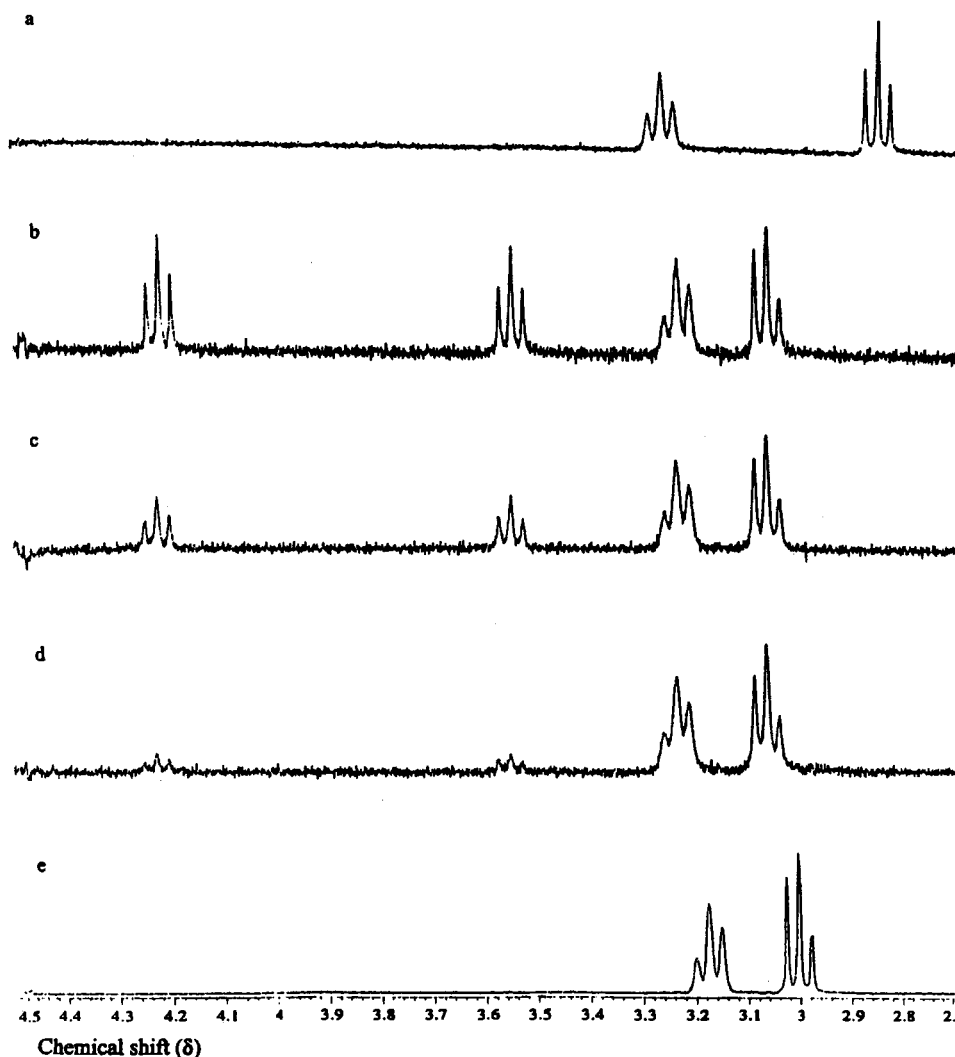
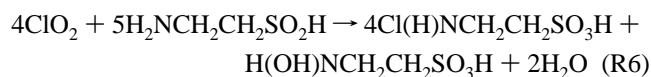


**Figure 2.**  $^1\text{H}$  NMR spectra of the reactants, intermediates, and products. (a) Standard spectrum of hypotaurine in  $\text{DClO}_4$  ( $\text{pH} < 3$ ). (b) Appearance of spectrum after mixing a 1:2 ratio of  $\text{ClO}_2^-$ : $\text{H}_2\text{NCH}_2\text{CH}_2\text{SO}_2\text{H}$ . The triplets observed at  $\delta = 3.55$  and  $4.22$  are due to an intermediate species,  $\text{ClHNCH}_2\text{CH}_2\text{SO}_2\text{H}$ , *N*-chlorohypotaurine. (c) Addition of more  $\text{ClO}_2^-$  to the mixture in (b) sees the progressive disappearance of the triplets at  $\delta = 3.55$  and  $4.22$ . (d) In excess  $\text{ClO}_2^-$  the peaks at  $\delta = 3.55$  and  $4.22$  disappear completely, leaving peaks characteristic of chlorotaurine. The same spectrum for chlorotaurine was observed in ref 23. (e) Spectrum of taurine in  $\text{DClO}_4$  inserted for comparison with the product spectrum in (d). NMR spectra of taurine and chlorotaurine are very similar (see ref 23).

intercept on the  $\text{ClO}_2^-$ -concentration axis. The intercept on this axis is concentration one needs to satisfy stoichiometry R4 without any excess  $\text{ClO}_2^-$  left to produce  $\text{ClO}_2$  as in reaction R5. Reaction R5 is a slow decomposition reaction whose end point is reached after several days and thus unreliable for the determination of this reaction's stoichiometry. The value of the intercept from these data clearly supports stoichiometry R4.

The stoichiometry of the  $\text{ClO}_2^-$ -hypotaurine reaction was determined by titration. A fixed amount of hypotaurine was titrated against standardized aqueous  $\text{ClO}_2$ , and the end point was determined as the point at which the yellow chlorine dioxide color no longer vanishes. The detection of the end point could be enhanced by the addition of freshly prepared starch solution with mercuric iodide as a preservative. Starch without mercuric iodide did not give a complex with  $\text{ClO}_2$ .<sup>28</sup> The titration exercise gave a  $\text{ClO}_2^-$ :hypotaurine stoichiometric ratio of 4:5. The products were more difficult to identify. NMR spectra confirmed the formation of *N*-chlorotaurine only. We thus inferred the following stoichiometry:



The oxime formed in (R6) can condense with another taurine molecule to form a tauryl dimer. NMR spectra could not give a distinctly different spectrum for the products of the  $\text{ClO}_2^-$ -hypotaurine reaction compared to the original spectrum of hypotaurine. The two triplet peaks did not shift from their original positions.

**Reaction Dynamics. The Induction Period.** The reaction of chlorite with hypotaurine was much faster than the corresponding reaction with taurine.<sup>1</sup> Reaction solutions displayed a finite induction period of between 10 and 1000 s (depending on initial conditions) before the formation of  $\text{ClO}_2$  in excess  $\text{ClO}_2^-$ :  $[\text{ClO}_2^-]_0 > [\text{H}_2\text{NCH}_2\text{CH}_2\text{SO}_2\text{H}]_0$ . No  $\text{ClO}_2$  formation is observed in excess hypotaurine. Figure 3a shows the effect of varying chlorite at constant acid and hypotaurine concentrations. Figure 3b shows that there is a linear dependence between the induction time and the inverse of the initial chlorite concentrations,  $[\text{ClO}_2^-]_0$ . At fixed hypotaurine concentrations, however, this linearity is lost at low chlorite concentrations (see Figure 3b). This is to be expected as we shall see from the data in Figure 5 and suggests that the precursor reaction to formation of  $\text{ClO}_2$  is dependent on the first power in the concentrations of  $\text{ClO}_2^-$ . In the range of acid strength,  $2.0 \times 10^{-2} \text{ M} > [\text{H}^+]_0$

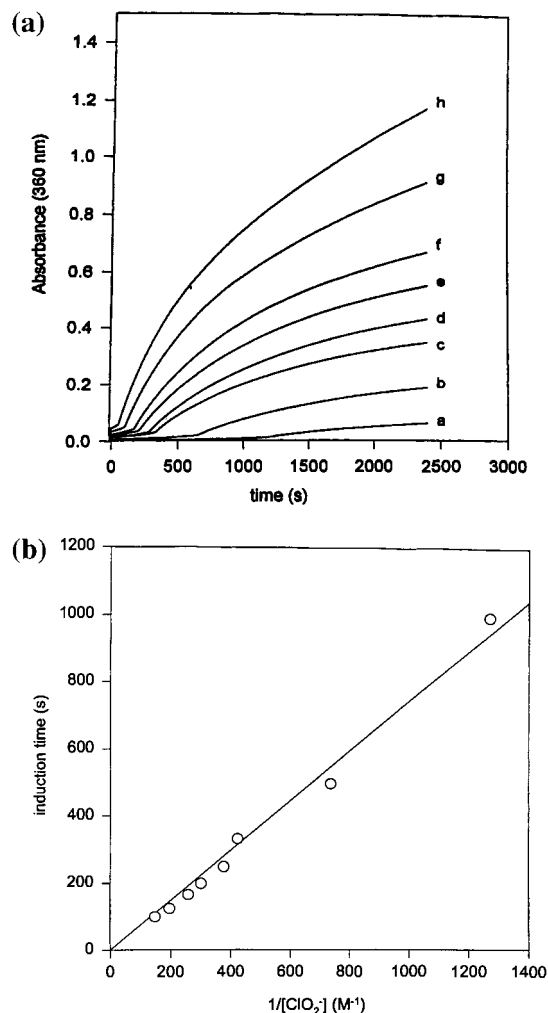


**Figure 3.** (a) Reaction dynamics in excess  $\text{ClO}_2^-$ . There is a progressive increase in the  $[\text{ClO}_2^-]_0$  in going from (a) to (h). As  $[\text{ClO}_2^-]_0$  increases, there is a shortening of the induction period and an increase in the rate of formation of the  $\text{ClO}_2$ .  $[\text{H}_2\text{NCH}_2\text{CH}_2\text{SO}_2\text{H}]_0 = 1.0 \times 10^{-3}$  M,  $[\text{H}^+]_0 = 0.050$  M.  $[\text{ClO}_2^-]_0 =$  (a)  $1.0 \times 10^{-3}$  M with increments of  $1.0 \times 10^{-3}$  M in (b) to (f); (g)  $8.0 \times 10^{-3}$  M, (h)  $1.0 \times 10^{-2}$  M. (b) Plot of the induction time vs the inverse of the chlorite concentration. The straight line indicates that the hypotaurine consumption reaction has first-order dependence with respect to the chlorite concentrations.

$> 1.0 \times 10^{-3}$  M, there is also a linear dependence of the induction period on the inverse of the acid concentration. Linearity is lost in highly acidic environments, as the experimental data become irreproducible with what appears to be a limiting effect. Figure 4 shows this effect within the linear region. As the acid concentrations are increased past 0.02 M, the induction period stays constant at about 310 s (from Figure 4), and as the acid concentrations are increased further, past 0.1 M, the induction period starts to increase, showing acid retardation at high acid concentrations.

The effect of varying hypotaurine concentrations also was complex. In high excess of  $\text{ClO}_2^-$ , such that ratio  $R = [\text{ClO}_2^-]_0 / [\text{H}_2\text{NCH}_2\text{CH}_2\text{SO}_2\text{H}]_0 > 4.0$ , variation of hypotaurine concentrations did not change the induction period of the reaction (see Figure 5), although it did affect the rate of formation of chlorine dioxide at the end of the induction period. Increasing the hypotaurine concentrations so that  $R < 4$  had the effect of increasing the induction period, as it now took much longer to oxidize the hypotaurine completely and allow the  $\text{ClO}_2$  to accumulate.

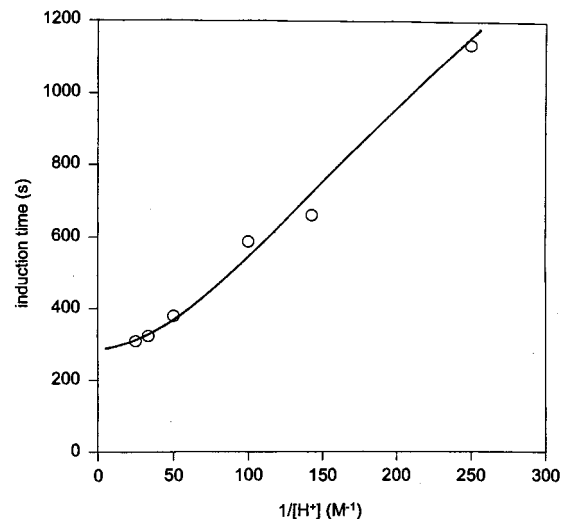


**Figure 4.** Dependence of the induction period on the acid concentrations. Acid is merely acting as a catalyst in this reaction. This plot is only valid within the narrow acid concentration range plotted.

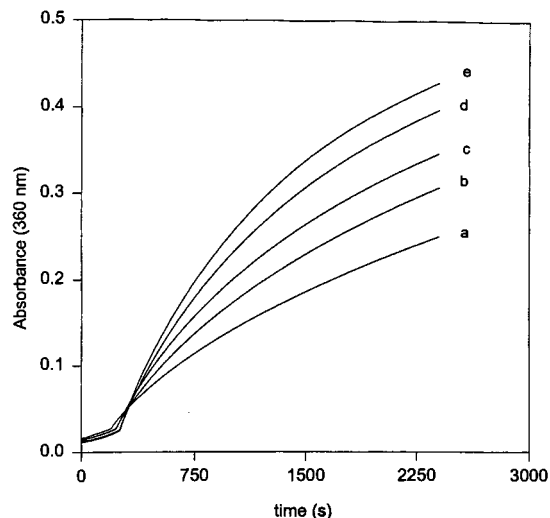


**Figure 5.** Reaction dynamics showing the "peacock-type" absorbance traces under conditions of  $[\text{ClO}_2^-]_0 \gg [\text{H}_2\text{NCH}_2\text{CH}_2\text{SO}_2\text{H}]_0$ .  $[\text{ClO}_2^-]_0 = 4.02 \times 10^{-3}$  M.  $[\text{H}_2\text{NCH}_2\text{CH}_2\text{SO}_2\text{H}]_0 =$  (a)  $2.0 \times 10^{-4}$  M, (b)  $4.0 \times 10^{-4}$  M, (c)  $6.0 \times 10^{-4}$  M, (d)  $8.0 \times 10^{-4}$  M, and (e)  $1.0 \times 10^{-3}$  M. The induction period gets longer as the hypotaurine concentrations are increased further. Though the induction period does not increase, the rate of formation of  $\text{ClO}_2$  increases with  $[\text{H}_2\text{NCH}_2\text{CH}_2\text{SO}_2\text{H}]_0$  (see plot shown in Figure 7b).

**Formation of Chlorine Dioxide.** The relationship between the initial reactant concentrations and the rate of formation of  $\text{ClO}_2$  at the end of the induction period can lead to information on the rate of formation of the reactive intermediates that control the formation of  $\text{ClO}_2$ . The log-log plot shown in Figure 6a was derived from the data shown in Figure 3a. Initial rates were estimated as the tangents of the chlorine dioxide formation curves. Only about 2% of the  $\text{ClO}_2$  formation data was used for each curve. The log-log plot gave a slope of  $0.94 \pm 0.07$ ; thus, the rate of formation of  $\text{ClO}_2$  has a first-order dependence on the initial concentration of the chlorite. At the end of the induction period the reagent concentrations, especially when  $[\text{ClO}_2^-]_0 \approx [\text{H}_2\text{NCH}_2\text{CH}_2\text{SO}_2\text{H}]_0$ , will be vastly different from the concentrations at the beginning of the reaction. The existence of a relationship between initial concentrations and the reaction rate at the beginning of the induction period indicates that the two processes (consumption of hypotaurine and formation of chlorine dioxide) are connected. The data in



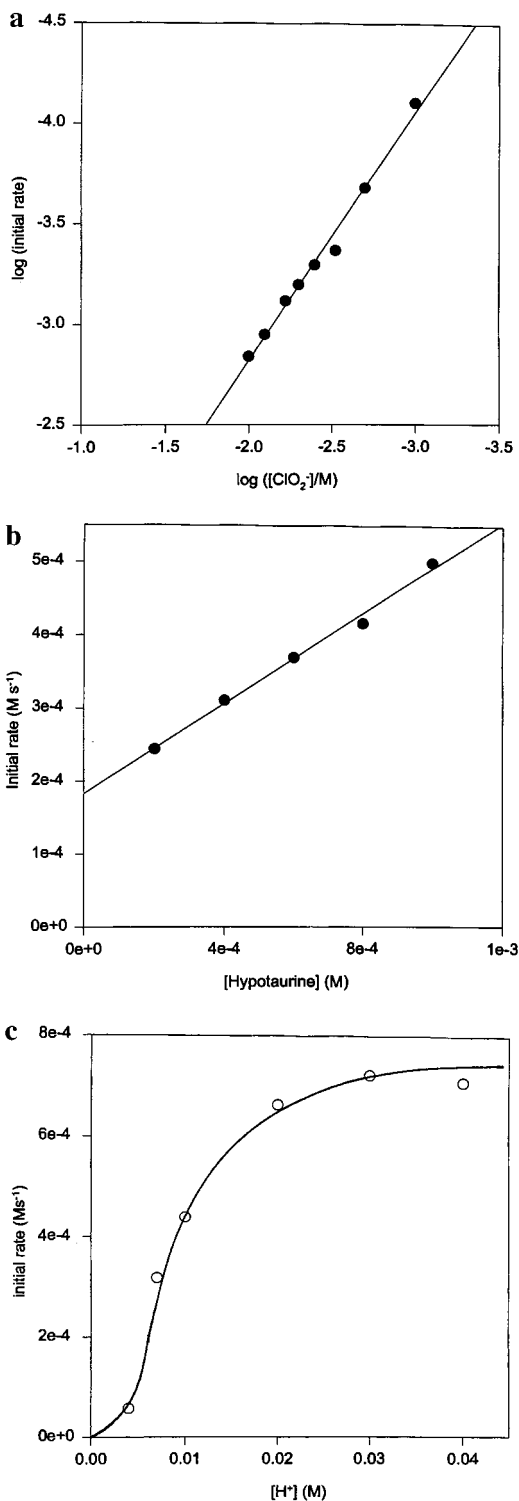


**Figure 6.** Plots showing the dependence of the  $\text{ClO}_2^-$ -formation on the initial reagent concentrations. (a) A log-log plot of chlorite concentrations against initial rate of formation of  $\text{ClO}_2$ . The slope of 1.0 confirms unit order with respect to  $[\text{ClO}_2^-]_0$ . Data used for this plot derived from data in Figure 4a. (b) The effect of the hypotaurine concentrations on the initial rate of formation of  $\text{ClO}_2$ . This is from data shown in Figure 6. (c) Complex dependence of the rate of formation of  $\text{ClO}_2$  with respect to acid. Plot shows a saturation as well as a retardation as the acid is increased further.

Figure 5 were also used to evaluate the plot shown in Figure 6b. The initial rate of formation of chlorine dioxide is also dependent to the first power on the initial hypotaurine concentrations. The positive intercept observed in Figure 6b is expected since even without the hypotaurine, formation of  $\text{ClO}_2$

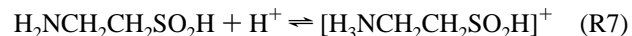
is expected from the standard decomposition of chlorite as shown in stoichiometry R5.<sup>27</sup> Figure 6c shows the complex dependence of the initial rate of formation of  $\text{ClO}_2$  on the acid concentrations. At low acid concentrations, there is a reasonably linear relationship between the rate and the acid concentrations, but by pH 2 there is a rapid saturation followed by a retardation of the reaction as the acid concentrations are further increased. This is the same type of effect observed in the data shown in Figure 4.

*The  $\text{ClO}_2$ - $\text{H}_2\text{NCH}_2\text{CH}_2\text{SO}_2\text{H}$  Reaction.* The interactions between hypotaurine and chlorine dioxide are crucial in determining the global reaction mechanism. How rapidly does  $\text{ClO}_2$  oxidize hypotaurine? If this process is slow (or nonexistent), then both  $\text{ClO}_2$  and hypotaurine can coexist in the reaction solution, and the induction period data cannot be effectively associated with any of the kinetics parameters we seek for the chlorite-hypotaurine reaction. A rapid  $\text{ClO}_2$ - $\text{H}_2\text{NCH}_2\text{CH}_2\text{SO}_2\text{H}$  reaction would indicate that any  $\text{ClO}_2$  formed during the induction period will be quickly mopped up by hypotaurine, and formation of  $\text{ClO}_2$  would then indicate complete consumption of the hypotaurine substrate.

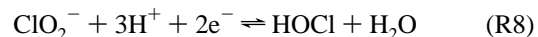
The  $\text{ClO}_2$ - $\text{H}_2\text{NCH}_2\text{CH}_2\text{SO}_2\text{H}$  reaction was found to be fast (Figure 7a,b), complete in typically less than 10 s. This can be compared with data shown in Figures 3a and 5 in which typical induction times of the chlorite-hypotaurine reaction are of the order of 100 s, and complete reaction may require over 3000 s. Thus, the rapid nature of the  $\text{ClO}_2$ - $\text{H}_2\text{NCH}_2\text{CH}_2\text{SO}_2\text{H}$  reaction simplifies deduction of a plausible mechanism from the reaction data. Figure 7a shows the effect of varying  $[\text{ClO}_2]_0$  at constant  $[\text{H}^+]_0$  and  $[\text{H}_2\text{NCH}_2\text{CH}_2\text{SO}_2\text{H}]_0$ ; the insert is a log-log plot of initial rates vs  $[\text{ClO}_2]_0$ , with a slope of  $1.06 \pm 0.11$ . Figure 7b shows the effect of varying hypotaurine; the insert shows the log-log plot, which gives a slope of  $0.98 \pm 0.05$ . The reactions involving oxidation by  $\text{ClO}_2$  were reproducible, and no special experimental precautions were needed for these sets of experiments.

### Mechanism

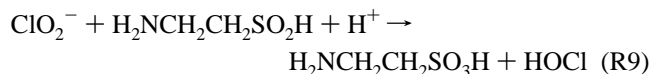
Hypotaurine has a  $\text{p}K_b$  of 9.56.<sup>29</sup> At the pH conditions utilized in these experiments, we expect the amino group to be fully protonated:



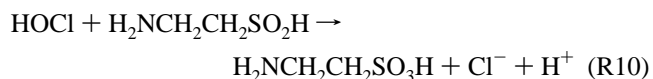
The first step in the mechanism is the formation of the active oxidizing species, HOCl. HOCl is formed by the two-equivalent reduction of  $\text{ClO}_2^-$ :



Initially, the only reductant is hypotaurine, and thus its oxidation is the initiation reaction:



The formation of HOCl in reaction R9 triggers several rapid reactions. HOCl can rapidly oxidize the remaining hypotaurine to taurine



or oxidize hypotaurine to *N*-chlorohypotaurine

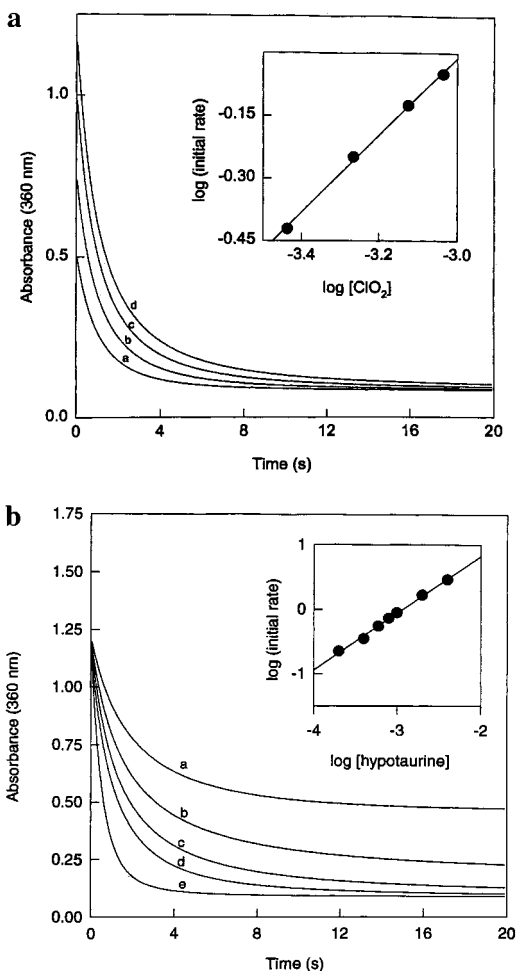
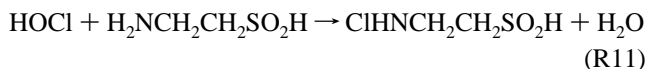
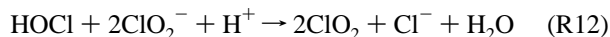


**Figure 7.** (a) Direct reaction of  $\text{ClO}_2$  with  $\text{H}_2\text{NCH}_2\text{CH}_2\text{SO}_2\text{H}$  in unbuffered solutions. The reaction is very fast. The insert shows a log–log plot of the  $[\text{ClO}_2]_0$  and initial rate of the reaction which gives a value of unity dependence of the reaction on  $[\text{ClO}_2]_0$ .  $[\text{H}_2\text{NCH}_2\text{CH}_2\text{SO}_2\text{H}]_0 = 1.0 \times 10^{-3}$  M.  $[\text{ClO}_2]_0 =$  (a)  $3.7 \times 10^{-4}$  M, (b)  $5.4 \times 10^{-4}$  M, (c)  $7.5 \times 10^{-4}$  M, (d)  $9.2 \times 10^{-4}$  M, and (e)  $1.8 \times 10^{-3}$  M. (b) Effect of hypotaurine concentrations on the  $\text{ClO}_2$ – $\text{H}_2\text{NCH}_2\text{CH}_2\text{SO}_2\text{H}$ . The insert shows a log–log plot of the data which also gives an order of 1.0 in  $[\text{H}_2\text{NCH}_2\text{CH}_2\text{SO}_2\text{H}]_0$ .  $[\text{ClO}_2]_0 = 9.2 \times 10^{-4}$  M. Ratio =  $[\text{ClO}_2]_0/[\text{H}_2\text{NCH}_2\text{CH}_2\text{SO}_2\text{H}]_0 =$  (a) 4.61, (b) 2.30, (c) 1.54, (d) 1.15, and (e) 0.92.



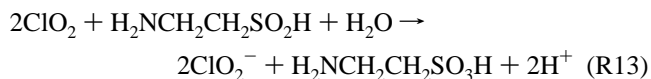
Oxyhalogen reactions will also be activated by formation of HOCl. The most important reaction is the formation of  $\text{ClO}_2$  from  $\text{ClO}_2^-$ :<sup>30</sup>



Unless there is a reaction that consumes  $\text{ClO}_2$  as rapidly as it is produced by reaction R12, we expect an almost instant accumulation of yellow  $\text{ClO}_2$  as soon as the reaction commences as has been observed in the oxidation of aldehydes by  $\text{ClO}_2^-$ .<sup>31</sup> Our kinetics data, e.g., Figures 3a and 5, show that the reaction exhibits a finite induction period in the formation of  $\text{ClO}_2$ . These induction periods can be up to thousands of seconds depending on initial conditions.

Apart from some of the oxyhalogen species, there are only two possible reductants in the reaction medium: hypotaurine and *N*-chlorohypotaurine. The reaction of taurine and  $\text{ClO}_2$  can be ignored since in a previous study, reaction mixtures of  $\text{ClO}_2$

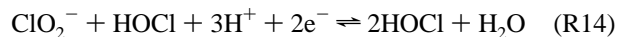
and taurine showed no tendency to react over long periods of time.<sup>23</sup> However,  $\text{ClO}_2$  can be consumed by reaction with hypotaurine:



Reaction R13 is fast enough to mop up all the  $\text{ClO}_2$  molecules as soon as they are formed from reaction R12. The data for reaction R13 are shown in Figure 7a,b where the reaction is 90% complete within 1.00 s. Reaction R13 is not an elementary step. The kinetics data clearly implicate bimolecular kinetics with orders of unity in the concentrations of chlorine dioxide and hypotaurine. The initial step of reaction R13 is a one-electron oxidation of hypotaurine to form an unstable radical organic species which rapidly reacts with more  $\text{ClO}_2$  to form taurine. The rate of the reaction was deduced to be

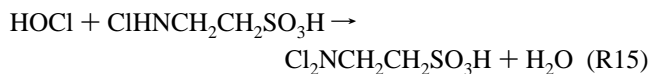
$$-d[\text{ClO}_2]/dt = k_0[\text{ClO}_2][\text{H}_2\text{NCH}_2\text{CH}_2\text{SO}_2\text{H}] \quad (1)$$

with  $k_0 = 801 \text{ M}^{-1} \text{ s}^{-1}$ . In excess chlorite, it has been established that the formation of HOCl from  $\text{ClO}_2^-$  is autocatalytic such that



The mechanism for the autocatalytic sequence described by the composite reaction R14 is well-known.<sup>32</sup> The expected rapidly increasing  $\text{ClO}_2$  concentrations (due to quadratic autocatalysis) are not observed due to limited concentrations of  $\text{ClO}_2^-$  and the fact that nonautocatalytic pathways for the consumption of HOCl, as in reactions R10 and R11, also contribute to the overall reaction dynamics.

**Product Formation.** The  $^1\text{H}$  NMR spectra shown in Figure 2 confirm that the reaction is quite complex, with a set of reactions that can be derived by permuting the set of oxidants in the reaction medium ( $\text{ClO}_2^-$ , HOCl, and  $\text{ClO}_2$ ) with the set of reductants ( $\text{H}_2\text{NCH}_2\text{CH}_2\text{SO}_2\text{H}$ ,  $\text{H}_2\text{NCH}_2\text{CH}_2\text{SO}_3\text{H}$ , and  $\text{ClHNCH}_2\text{CH}_2\text{SO}_2\text{H}$ ). The NMR data could not give evidence of further oxidation of *N*-chlorotaurine to dichlorotaurine because the NMR spectra of both the mono- and dichloro compounds are very similar:



The stoichiometry of the reaction, however, clearly indicates monochlorotaurine as the overwhelmingly favored product. Dichlorotaurine is favored in highly acidic environments.<sup>33</sup> Our experiments were carried out under mildly acidic conditions, hence the dominance of the monochlorotaurine product.

**Explanation of Acid Dependence.** Linear acid dependence with respect to the induction period and rate of formation of chlorine dioxide is obtained within a narrow range of acid concentrations,  $0.005 \text{ M} < [\text{H}^+] < 0.02 \text{ M}$ . Protonation can occur at the nitrogen group of the hypotaurine as in reaction R7. Protonation of  $\text{ClO}_2^-$  can also occur, with Cl(III) existing as either the protonated  $\text{HClO}_2$  form or unprotonated  $\text{ClO}_2^-$  anion:



Since the  $\text{pK}_a$  of chlorous acid is about 2.5,<sup>34</sup> Cl(III) species below  $\text{pH} = 2.5$  exist predominantly as  $\text{HClO}_2$ .

**TABLE 1: Reactions Used in the Simulation of the  $\text{ClO}_2^- - \text{H}_2\text{NCH}_2\text{CH}_2\text{SO}_2\text{H}$  Reaction**

no.	reaction
M1	$\text{ClO}_2^- + \text{H}^+ \rightleftharpoons \text{HClO}_2$
M2	$\text{H}_2\text{NCH}_2\text{CH}_2\text{SO}_2\text{H} + \text{H}^+ \rightarrow [\text{H}_3\text{NCH}_2\text{CH}_2\text{SO}_2\text{H}]^+$
M3	$\text{ClO}_2^- + \text{H}_2\text{NCH}_2\text{CH}_2\text{SO}_2\text{H} + \text{H}^+ \rightarrow \text{H}_2\text{NCH}_2\text{CH}_2\text{SO}_3\text{H} + \text{HOCl}$
M4	$\text{ClO}_2^- + \text{H}_2\text{NCH}_2\text{CH}_2\text{SO}_3\text{H} + \text{H}^+ \rightarrow \text{H}(\text{OH})\text{NCH}_2\text{CH}_2\text{SO}_3\text{H} + \text{HOCl}$
M5	$\text{HOCl} + \text{H}(\text{OH})\text{NCH}_2\text{CH}_2\text{SO}_2\text{H} + \text{H}_2\text{O} \rightarrow \text{H}(\text{OH})\text{NCH}_2\text{CH}_2\text{SO}_3\text{H} + \text{H}^+ + \text{Cl}^-$
M6	$\text{H}(\text{OH})\text{NCH}_2\text{CH}_2\text{SO}_3\text{H} + \text{H}^+ + \text{Cl}^- \rightarrow \text{Cl}(\text{H})\text{NCH}_2\text{CH}_2\text{SO}_3\text{H} + \text{H}_2\text{O}$
M7	$\text{HOCl} + \text{H}_2\text{NCH}_2\text{CH}_2\text{SO}_2\text{H} \rightarrow \text{H}_2\text{NCH}_2\text{CH}_2\text{SO}_3\text{H} + \text{Cl}^- + \text{H}^+$
M8	$\text{HOCl} + 2\text{ClO}_2^- + \text{H}^+ \rightarrow 2\text{ClO}_2(\text{aq}) + \text{Cl}^- + \text{H}_2\text{O}$
M9	$2\text{ClO}_2(\text{aq}) + \text{H}_2\text{NCH}_2\text{CH}_2\text{SO}_2\text{H} + \text{H}_2\text{O} \rightarrow 2\text{ClO}_2^- + \text{H}_2\text{NCH}_2\text{CH}_2\text{SO}_3\text{H} + 2\text{H}^+$
M10	$\text{HOCl} + \text{H}_2\text{NCH}_2\text{CH}_2\text{SO}_3\text{H} + \text{H}_2\text{O} \rightarrow \text{H}(\text{OH})\text{NCH}_2\text{CH}_2\text{SO}_3\text{H} + \text{Cl}^- + \text{H}^+$
M11	$\text{ClO}_2^- + \text{Cl}(\text{H})\text{NCH}_2\text{CH}_2\text{SO}_2\text{H} + \text{H}^+ \rightarrow \text{Cl}(\text{H})\text{NCH}_2\text{CH}_2\text{SO}_3\text{H} + \text{HOCl}$
M12	$\text{HOCl} + \text{Cl}(\text{H})\text{NCH}_2\text{CH}_2\text{SO}_2\text{H} \rightarrow \text{Cl}(\text{H})\text{NCH}_2\text{CH}_2\text{SO}_3\text{H} + \text{Cl}^- + \text{H}^+$
M13	$2\text{Cl}(\text{H})\text{NCH}_2\text{CH}_2\text{SO}_3\text{H} + \text{H}^+ \rightleftharpoons \text{Cl}_2\text{NCH}_2\text{CH}_2\text{SO}_3\text{H} + [\text{H}_3\text{NCH}_2\text{CH}_2\text{SO}_2\text{H}]^+$

**TABLE 2: Rate Laws and Rate Constants Used in Computer Simulations**

reaction	forward reaction	reverse reaction
M1	$1.0 \times 10^{10}[\text{H}^+][\text{ClO}_2^-]$	$3.16 \times 10^7[\text{HClO}_2]$
M2	$5.0 \times 10^8[\text{H}_2\text{NCH}_2\text{CH}_2\text{SO}_2\text{H}][\text{H}^+]$	$1.0 \times 10^7[[\text{H}_3\text{NCH}_2\text{CH}_2\text{SO}_2\text{H}]^+]$
M3	$5.0 \times 10^2[\text{ClO}_2^-][\text{H}_2\text{NCH}_2\text{CH}_2\text{SO}_2\text{H}][\text{H}^+]$	
M4	$55[\text{ClO}_2^-][\text{H}_2\text{NCH}_2\text{CH}_2\text{SO}_3\text{H}][\text{H}^+]$	
M5	$1.0 \times 10^3[\text{HOCl}][\text{H}(\text{OH})\text{NCH}_2\text{CH}_2\text{SO}_2\text{H}]$	
M6	$1.0 \times 10^6[\text{H}(\text{OH})\text{NCH}_2\text{CH}_2\text{SO}_2\text{H}][\text{Cl}^-][\text{H}^+]$	
M7	$1.5 \times 10^3[\text{HOCl}][\text{H}_2\text{NCH}_2\text{CH}_2\text{SO}_3\text{H}]$	
M8	$1.06 \times 10^6[\text{HOCl}][\text{ClO}_2^-][\text{H}^+]$	$1.0 \times 10^2[\text{ClO}_2]^2[\text{Cl}^-]$
M9	$8.01 \times 10^2[\text{ClO}_2][\text{H}_2\text{NCH}_2\text{CH}_2\text{SO}_2\text{H}]$	
M10	$1.1 \times 10^3[\text{HOCl}][\text{H}_2\text{NCH}_2\text{CH}_2\text{SO}_3\text{H}]$	
M11	$1.5 \times 10^2[\text{ClO}_2^-][\text{Cl}(\text{H})\text{NCH}_2\text{CH}_2\text{SO}_2\text{H}][\text{H}^+]$	
M12	$1.0 \times 10^3[\text{HOCl}][\text{Cl}(\text{H})\text{NCH}_2\text{CH}_2\text{SO}_2\text{H}][\text{H}^+]$	
M13	$5.0 \times 10^6[\text{Cl}(\text{H})\text{NCH}_2\text{CH}_2\text{SO}_3\text{H}]^2[\text{H}^+]$	$1.0 \times 10^4[\text{Cl}(\text{H})\text{NCH}_2\text{CH}_2\text{SO}_3\text{H}][[\text{H}_3\text{NCH}_2\text{CH}_2\text{SO}_3\text{H}]^+]$

In this reaction system, the formation of HOCl is the rate-determining step giving the rate of reaction as

$$-\text{d}[\text{H}_2\text{NCH}_2\text{CH}_2\text{SO}_2\text{H}]/\text{d}t = k_1[\text{ClO}_2^-][\text{H}_2\text{NCH}_2\text{CH}_2\text{SO}_2\text{H}][\text{H}^+] \quad (2)$$

$\text{ClO}_2^-$  is a better nucleophile than  $\text{HClO}_2$  and would react much faster with hypotaurine and/or protonated hypotaurine.  $\text{HClO}_2$  is not completely unreactive, but it reacts slowly with hypotaurine. Thus, no simple approximations could be made to evaluate  $k_1$ . Taking into account the equilibrium shown in reaction R16, the rate of reaction R9 will be given by

$$-\text{d}[\text{H}_2\text{NCH}_2\text{CH}_2\text{SO}_2\text{H}]/\text{d}t = k_1[\text{Cl}(\text{III})]_{\text{T}}[\text{H}_2\text{NCH}_2\text{CH}_2\text{SO}_2\text{H}][\text{H}^+]/(1 + K_a[\text{H}^+]) \quad (3)$$

where  $[\text{Cl}(\text{III})]_{\text{T}} = [\text{ClO}_2^-] + [\text{HClO}_2]$  and  $K_a$  is the acid dissociation constant for chlorous acid. Thus, simple first-order kinetics in acid will be expected at low acid concentrations. As acidity increases, one will notice a saturation followed by a retardation. This is illustrated in the data shown in Figure 6c.

**Computer Simulations.** The reaction network used to simulate the reaction system is shown in Table 1. The rate laws and rate constants used in the simulations are shown in Table 2. Only one oxyhalogen reaction (reaction M8) and two protolytic reactions (reactions M1 and M2) were used. The remaining 10 reactions were interactions between an oxyhalogen species and one of the four possible amino acid species in solution. Reaction M1 was needed to explain the acid retardation that is observed in pH conditions lower than the  $\text{p}K_a$  of chlorous acid (see Figure 6c). The kinetics parameters used for this reaction were taken from the work of Epstein et al.<sup>35</sup> Lower rate constants could be used for (M1) as long as the  $\text{p}K_a$  was maintained at 2.5. Higher rate constants for (M1) rendered the simulations stiff with the simulations not giving any better fit to the data. If, as is assumed in the proposed mechanism,

$\text{HClO}_2$  is slower reacting (cf. reactions M3 and M4), then the acid retardation can be justified from the increase in the slower-reacting form of Cl(III) species as acid concentrations are increased. Reaction M2 was not important in influencing the rate of reaction since the protonated species was dominant at the pH conditions used for these experiments. High rate constants for both the forward and reverse reactions of reaction M2 made it unimportant in determining the overall global dynamics of the reaction. Reaction M3 was important since it is the reaction initiator which produces the reactive intermediate, HOCl. Reaction M3 could be split into two reactions in which the initial products are taurine and  $\text{OCl}^-$ .  $\text{OCl}^-$  is then quickly protonated to form HOCl. The addition of another rapid protolytic reaction,  $\text{H}^+ + \text{OCl}^-$ , however, made the integration extremely stiff, also without any improvement in the results obtained. Reaction M4 is also an initiator reaction in which the oxidation occurs at the nitrogen center. Reactions M6 + M10 can be combined to give reaction R11 in which the chlorotaurine is formed directly without formation of  $\text{Cl}^-$ . The use of (R12) instead of (M6) + (M10) did not give a better fit to the data. We assumed that all chlorine dioxide is formed in reaction M8 and is consumed only in (M9). The other route for the consumption of chlorine dioxide is the reverse reaction of (M8). This route could have been important in high  $\text{Cl}^-$  concentrations, but in these simulations,  $\text{Cl}^-$  concentrations never rose above  $10^{-6}$  M since reaction M6 instantly consumed all the chloride formed in the reaction.

**Estimation of Some of the Rate Constants. Reaction M3.** The final value used was estimated from the best fit to the induction period. This estimation could be made by modeling a network of reactions M3 + M8 + M9. The rough value obtained could then be refined to fit the overall reaction data.

**Reaction M4.** This was estimated from Chinake et al. (ref 1, part 22). In this reference, taurine was reacted with chlorite. The chlorine dioxide formed was unreactive toward taurine, and so the rate of formation of  $\text{ClO}_2$  in this reaction gave a good

estimate of the  $\text{ClO}_2^-$ -taurine reaction after accounting for the stoichiometric factors.

**Reaction M5.** This reaction's rate constant was initially estimated from the data in Figure 2. The rate at which the two spurious triplets ( $\delta = 4.22$  and  $3.55$ ) disappear gives a good estimate of the rate of consumption of  $\text{H}(\text{OH})\text{NCH}_2\text{CH}_2\text{SO}_2\text{H}$  and  $\text{Cl}(\text{H})\text{NCH}_2\text{CH}_2\text{SO}_2\text{H}$ .

**Reaction M6.** This reaction was assumed to be fast and not rate determining. The chosen value of  $1.0 \times 10^6 \text{ M}^{-2} \text{ s}^{-1}$  was sufficient to allow it to consume the  $\text{Cl}^-$  ions as soon as they are formed.

**Reaction M7.** The initial guess value for the kinetics parameters for this reaction was made by running a crude  $\text{Br}_2^-$ -hypotaurine stopped-flow study ( $\lambda = 390 \text{ nm}$ ). In general, the  $\text{Cl}_2$  and  $\text{HOCl}$  oxidations are slightly faster than the corresponding bromine analogues.

**Reaction M8.** Rate constants were taken directly from the work of Peintler et al.<sup>35</sup>

**Reaction M9.** Rate constants were estimated directly from this study.

**Reaction M10.** Rate constants were estimated from our recent work on the bromine-*taurine* reaction.<sup>36</sup>

**Reactions M11 and M12.** These were purely guessed and were not important in determining the overall global dynamics of the reaction system.

**Reaction M13.** This reaction was only important for stoichiometric consistency and did not affect the reaction dynamics.<sup>33</sup> Our stoichiometric determinations showed that very little dichlorotaurine is formed, and so the equilibrium of reaction M13 was pushed to the left.

**Results of the Simulations.** The results of the simulations are shown in Figure 8a,b. The data shown in Figure 7b on the direct reaction between  $\text{ClO}_2^-$  and hypotaurine are modeled in Figure 8a. The mechanism in Table 1 could be used to generate the simulations shown in Figure 8a, but a much faster and more accurate simulations set could be obtained from the use of reactions M1, M2, M3, M5, M9, and M13 only. For these sets of simulations, the experimentally determined rate constant for reaction M9 was the most important. The kinetics parameters for reactions M1 and M2 were not important as long as they represented rapid equilibria in both directions. Data in Figure 5 were simulated in Figure 8b. These simulations could be generated by considering only three important reactions in the mechanism: (a) consumption of hypotaurine, reaction R4; (b) formation of chlorine dioxide, reaction M8; and (c) consumption of chlorine dioxide, reaction M9. Reaction M3 was then added to enhance reaction M8. Such a small set of reactions could easily predict the induction period and the rate of formation of chlorine dioxide. Acid dependence could then be simulated by addition of reactions M1 and M2.  $\text{ClO}_2^-$  oxidations are characterized by autocatalysis in  $\text{HOCl}$ <sup>37</sup> mediated via the intermediate  $\text{Cl}_2\text{O}_2$ . Reaction M8 can be split to show that  $\text{ClO}_2^-$  is produced via quadratic autocatalysis in  $\text{HOCl}$ . The rapid  $\text{ClO}_2^-$ -hypotaurine reaction made it unnecessary to include this autocatalytic step in the overall reaction mechanism. For the purposes of what we needed to prove, the mechanism in Table 1 appears to be adequate in describing the reaction of hypotaurine with chlorite.

## Conclusion

These experiments have shown that hypotaurine is much more active than taurine and can better be classified as an antioxidant. Taurine does not seem to be effective as an antioxidant for many of the common chemicals that attack physiological tissue, except

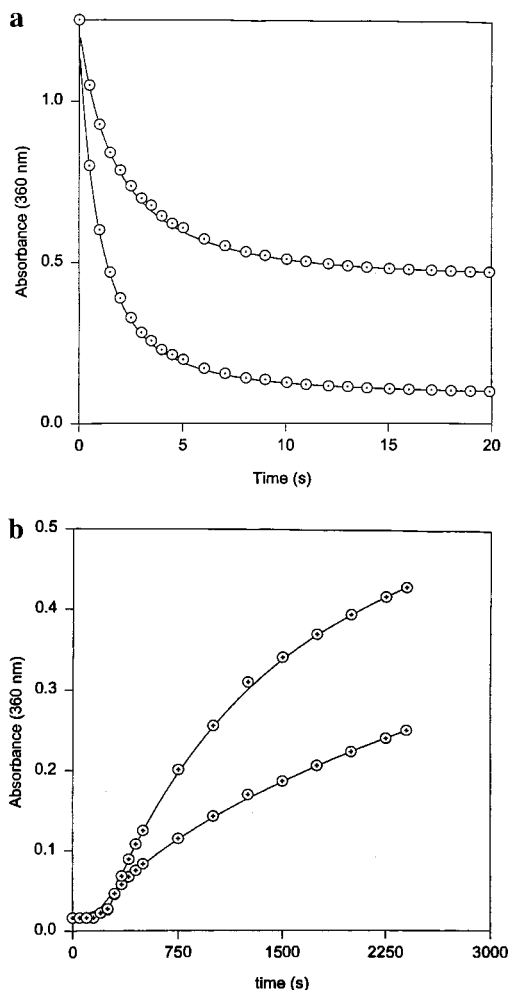


**Figure 8.** (a) Computer simulations of the  $\text{ClO}_2^-$ -hypotaurine reaction using the mechanism shown in Table 1. For these simulations, initial chlorite concentrations were set to zero.  $[\text{ClO}_2^-]_0 = 9.2 \times 10^{-4} \text{ M}$ . Ratio  $= [\text{ClO}_2^-]_0/[\text{H}_2\text{NCH}_2\text{CH}_2\text{SO}_2\text{H}]_0 =$  (a) 4.61 and (b) 0.92. Modeling that "peacock-type" absorbance traces shown in Figure 5. There is good agreement between the model and the experimental data especially with respect to the induction period and the rate of formation of chlorine dioxide after the induction period.

for  $\text{HOCl}$  and  $\text{HOBr}$ . For effective antioxidant activity, the compound must quickly detoxify the common oxidants to protect tissue. Taurine does not seem to be able to do this, but hypotaurine does. Any reactions of hypotaurine will take it to the more stable and relatively unreactive taurine. It is not clear how or whether hypotaurine can be regenerated after being converted to taurine. The fact that it is in the metabolic pathway may be sufficient to maintain its concentrations in physiological environments.

**Acknowledgment.** We thank University of Natal for granting sabbatical to B.S.M. This work was supported by research grant CHE 9632592 from the National Science Foundation.

## References and Notes

- (1) Part 23 in the series: Nonlinear Dynamics in Chemistry Derived from Sulfur Chemistry. Part 22: Chinake, C. R.; Simoyi, R. H. "Oxyhalogen-Sulfur Chemistry: Oxidation of Taurine by Chlorite in Acidic Medium". *J. Phys. Chem. A* **1997**, *101*, 1207.
- (2) Huxtable, R. A. *Physiol. Rev.* **1992**, *72*, 101.
- (3) Halliwell, B. *Biochem. Pharmacol.* **1995**, *49*, 1341.
- (4) Halliwell, B. *Free Radical Res. Commun.* **1990**, *9*, 1.
- (5) Gutteridge, J. M. C.; Stocks, J. *Crit. Rev. Clin. Lab. Sci.* **1981**, *14*, 257.



- (6) Halliwell, B.; Gutteridge, J. M. C. *Methods Enzymol.* **1990**, *186*, 1.
- (7) Thomas, E. L.; Grisham, M. B.; Jefferson, M. M. *J. Clin. Invest.* **1983**, *72*, 441.
- (8) Thomas, E. L.; Grisham, M. B.; Melton, D. F.; Jefferson, M. M. *J. Biol. Chem.* **1985**, *260*, 332.
- (9) Test, S. T.; Lampert, M. B.; Ossanna, Thoene, J. G.; Weiss, S. J. *J. Clin. Invest.* **1984**, *74*, 1341.
- (10) Jesaitis, A. J.; Dratz, E. A. *The Molecular Basis of Oxidative Damage by Leukocytes*; CRC Press: Boca Raton, FL, 1992.
- (11) Weiss, S. J. *New England J. Med.* **1989**, *320*, 365.
- (12) Mandel, G. L.; Sande, M. A. Penicillins, Cephalosporins and other Beta-Lactam Antibiotics. In *Pharmacological Basis of Therapeutics*, 7th ed.; Goodman, A., Gilman, A., Goodman, L. S., Rall, T. W., Murad, F., Eds.; McMillan: New York, 1985; p 1115.
- (13) Lapenna, D.; Cellini, L.; De Gioia, S.; Mezzetti, A.; Ciofani, G.; Festi, D.; Cuccurullo, F. *Biochem. Pharmacol.* **1995**, *49*, 1249.
- (14) Ogasawara, M.; Nakamura, T.; Koyama, I.; Nemoto, M.; Yoshida, T. *Chem. Pharm. Bull.* **1993**, *41*, 2172.
- (15) Yazdanbakhsh, M.; Eckmann, C. M.; Roos, D. *Am. J. Trop. Med. Hyg.* **1987**, *37*, 106.
- (16) Dolara, P.; Marino, P.; Buffoni, F. *Biochem. Pharmacol.* **1973**, *22*, 2085.
- (17) Crawford, J. M. *Biochem. Pharmacol.* **1963**, *12*, 1448.
- (18) Krough, A. *Osmotic Regulation in Aquatic Animals*; Cambridge University Press: Cambridge, 1939; p 56.
- (19) Meister, A. *Biochemistry of the Amino Acids*, 2nd ed.; Academic Press: New York, 1965; p 757.
- (20) Aruoma, O. I.; Halliwell, B.; Hoey, B. M.; Butler, J. *J. Biol. Chem.* **1984**, *256*, 251.
- (21) Fellman, J. H.; Roth, E. S. In *Biological Actions and Clinical Perspectives in Taurine*; Roth, E. S., Ed.; A. R. Liss: New York, 1985; p 71.
- (22) Weiss, S. J.; Lampert, M. B.; Test, S. T. *Science* **1983**, *222*, 625.
- (23) Reference 1 and Streete, K.; Mundoma, C.; Simoyi, R. H. *J. Phys. Chem. A*, submitted for publication.
- (24) Lengyel, I.; Rabai, Gy.; Epstein, I. R. *J. Am. Chem. Soc.* **1990**, *112*, 9104.
- (25) Indelli, A. J. *J. Phys. Chem.* **1964**, *68*, 3027.
- (26) Antelo, J. M.; Arce, F.; Campos, J.; Parajo, M. *Int. J. Chem. Kinet.* **1996**, *26*, 396.
- (27) Gordon, G.; Kieffer, R. G.; Rosenblatt, D. H. *Prog. Inorg. Chem.* **1972**, *15*, 201.
- (28) Chinake, C. R.; Simoyi, R. H. *J. Phys. Chem.* **1994**, *98*, 4012.
- (29) Jacobsen, J. G.; Smith, L. H. *Physiol. Rev.* **1968**, *48*, 424.
- (30) Taube, H.; Dodgen, H. *J. Am. Chem. Soc.* **1949**, *71*, 3330.
- (31) Isabell, H.; Sniegowski, L. T. *J. Res. Nat. Bur. Stand. (U.S.)* **1964**, *68A*, 301.
- (32) Salem, M.; Chinake, C. R.; Simoyi, R. H. *J. Phys. Chem.* **1996**, *100*, 9377.
- (33) Lin, Y. Y.; Write, C. E.; Zagorski, M.; Nakanishi, K. *Biochim. Biophys. Acta* **1988**, *969*, 242.
- (34) Atkins, P. W.; Beran, J. A. *General Chemistry*, 2nd ed.; Scientific American Books: New York, 1990; p 550.
- (35) Epstein, I. R.; Kustin, K.; Simoyi, R. H. *J. Phys. Chem.* **1992**, *96*, 5852.
- (36) Streete, K.; Mundoma, C.; Simoyi, R. H. *J. Phys. Chem. A*, submitted for publication.
- (37) Horvath, M.; Lengyel, I.; Bazsa, G. *Int. J. Chem. Kinet.* **1988**, *20*, 687.